Observations and Implications of Natural Laminar Flow on Practical Airplane Surfaces

B. J. Holmes
NASA Langley Research Center, Hampton, Virginia
and
C. J. Obara
Kentron International, Inc., Hampton, Virginia

Nomenclature

b = wing span, ft
c = airfoil chord, ft
C_x = section lift coefficient
C_l = trimmed airplane lift coefficient, $(W/S)/q_\infty$
C_d = section drag coefficient
C_p = pressure coefficient, $(p_l - p_\infty)/q_\infty$
D = propeller diameter, ft
h = amplitude of surface waviness, in.
h = density altitude, ft (mean sea level)
J = advance ratio, V/nD
M = freestream Mach number
n = propeller rotation, rpm
p = static pressure, psf
q = dynamic pressure, psf
r = leading-edge radius, in.
R = Reynolds number based on freestream conditions and local airfoil chord
R_t = Reynolds number based on freestream conditions and longitudinal length to transition
R_x = unit Reynolds number based on freestream conditions, ft^{-1}
R_θ = attachment line boundary-layer momentum thickness Reynolds number based on freestream conditions and leading-edge radius normal to the leading edge
s = distance along the surface from the leading edge
S = reference wing area, ft
t/c = airfoil thickness ratio
u = local velocity in boundary layer, ft/s
u_e = velocity at boundary-layer edge, ft/s
V = true airspeed, knots
V_c = calibrated airspeed, knots
W = airplane gross weight, lb
x = longitudinal dimension, ft
y = lateral dimension, ft
z = vertical dimension, ft
δ = boundary-layer thickness, in.
δ_e = canard flap (or elevator) deflection, deg
λ = wavelength measured in freestream direction, in.
Λ = leading-edge sweep angle, deg
η = nondimensional semispan location, $y/(b/2)$

Subscripts

$\bar{c}$ = mean aerodynamic chord
l = local point on airfoil
l.e. = leading edge
t = transition
u.s. = upper surface
∞ = freestream conditions

Abbreviations

GA(W) = general aviation (Whitcomb)
LS = low speed
NLF = natural laminar flow
rpm = revolutions per minute
T-S = Tollmien-Schlichting

Introduction

THE application of natural laminar flow (NLF) for viscous drag reduction on production powered airplanes has been precluded in the past by the aeronautical community consensus that NLF could be neither achieved nor maintained on practical surfaces subjected to typical operating environments. NLF is achieved on airfoil surfaces with small sweep by the design of long runs of favorable pressure

Dr. Holmes has been employed by the NASA Langley Research Center Low Speed Aerodynamics Division since 1974. During that time he has gained broad flight and wind-tunnel research experience on subsonic aerodynamic topics, including natural laminar flow, agricultural aviation, winglets, and advanced wing designs. Dr. Holmes' recent research has led to a new appreciation of the operational feasibility of achieving and maintaining natural laminar flow on modern airplanes. In addition, he has identified the potential performance and fuel efficiency gains available through cruise optimization of a new class of high-performance, single-engine business airplanes currently under development by industry. He is presently continuing his work at Langley in the area of viscous drag reduction. His undergraduate and graduate degrees in Aerospace Engineering were obtained at the University of Kansas.

Clifford Obara is employed as an aerodynamics engineer at Kentron International. He has been involved with the in-flight measurement, analysis, and documentation of aircraft performance and efficiency for 3 years. He has a B.S. in Mechanical Engineering from the Florida Institute of Technology and has concentrated most of his research in low-speed aerodynamics with emphasis on the application of natural laminar flow. Mr. Obara is a member of AIAA.

Submitted Aug. 9, 1982; presented as Paper ICAS-82-5.1.1 at the 13th Congress of ICAS and AIAA Aircraft Systems and Technology Conference, Seattle, Wash., Aug. 22-27, 1982; revision received May 19, 1983.

Table 1 Natural laminar

Principal investigators	Ref(s).	Airplane	Airfoil	Type of surface
Stüper	2	Klemm L26Va		Sanded plywood glove
Jones, Stephens,	3,4	Snark L6103	t/c= 17.5%	Sanded plywood glove
Haslam		Hart K1442	10%	Metal glove
Young, Morris	5,6	Anson	NACA 2218	Metal glove
		Courier	NACA 2219	Metal glove
Young, Serby, Morris	7	Battle	NACA 2417	Metal glove Production metal Wing surface Camouflage
Goett, Bicknell	8	Fairchild 22	N-22	Stiffened metal test panel
Bicknell	9	Northrup A-17A	NACA 2414.5	Production metal wing[c] Metal glove
Wetmore, Zalovcik, Platt	10	Douglas B-18	NACA 35-215	Wood glove
Zalovcik	11	XP-51	NACA $64_1$2-(1.4), (13.5)	Production metal surface[d]
Serby, Morgan, Cooper	12	Hawcon	(t/c) = 14% 25%	Wood glove Metal glove
Serby, Morgan	13	Heinkel He.70		Production wood surface
Tani	14	Japanese biplane		Wood glove
Zalovcik	15	Several aircraft	8 airfoils	Smoothed and gloved surfaces
Zalovcik, Skoog	16	XP-47F	NACA 66(215)-1 (16.5),α = 1.0 67(115)-213, a = 0.7	Production metal surface Smoothed surface
Zalovcik	17	P-47D	Republic S-3 (t/c) = 11%, 14.6%	Smoothed surfaces
Zalovcik, Daum	18	P-47D	Republic S-3	Production metal surface w/camouflage paint
Plascott, Higton, Smith	19,20	Hurricane II	NPL (t/c) = 14.8-17.9%	Smoothed surfaces
Smith, Higton	21	King Cobra	NACA 662x-116 662×-216	Production metal surface Smoothed surface
Britland	22	Vampire	NACA 67, 1-314, a = 1.0	Metal glove
Davies	23	Several aircraft		Production surface Smoothed surfaces
Gray, Davies	22	King Cobra	NACA 662x-116 661x-216	Smoothed surfaces
Montoya	25	F-111/ TACT	Super-critical NLF	Glove
Banner, McTigue, Petty	26	F-104	Biconvex (t/c) = 3.4%	Production metal Fiberglass glove surfaces

[a] Outside propeller slipstream. [b] Downstream of predicted laminar slipstream. [c] Flush rivets, aft-facing lap joint at x/c = 8%
[d] Various surface conditions.

low flight experiments

Speed or chord Reynolds no.	Measurements	Results	Comments
4.88×10^6	$C_p, u/u_e$	$(x/c)_t > 30\%$	First in-flight transition measurement
$2.8\text{-}10.8\times10^6$	$C_d, C_p, u/u_e$	$16\% < (x/c)_t < 30\%$	Waviness measured Effects of steps on transition measured
139 kts 122 kts	u/u_e u/u_e	$(x/c)_t = 17\%$ $(x/c)_t = 25\%$ [a]	Measurements inside and outside propeller slipstream
$12\text{-}18\times10^6$	$C_d, C_p, u/u_e$	$(x/c)_t = 18\%$ on glove	Drag of rivets and lap joints measured No effect of camouflage paint on transition No appreciable NLF on production surface
$3.9\text{-}4.6\times10^6$	$C_d, C_p, u/u_e$	$(x/c)_t = 37\%$ [b]	Proximate transition locations for flight and 30×60 ft wind tunnel
15×10^6	$C_d, C_p, u/u_e$	$(x/c)_t = 17.5\%$ (glove)	No appreciable NLF on production surface
30×10^6	$C_d, C_p, u/u_e$	$(x/c)_t = 42.4\%$	Waviness measured Engine operation effects measured
16×10^6	$C_d, C_p, u/u_e$		Waviness measured No appreciable NLF on production surface
8×10^6	$C_d, C_p, u/u_e$	$30\% < (x/c)_t < 40\%$	
16×10^6	C_d	$C_{d_{min}} = 0.0065$	
$5\text{-}10\times10^6$	$C_d, C_p, u/u_e$	$40\% < (x/c)_t < 51\%$	
$4\text{-}32\times10^6$	$C_d, C_p, u/u_e$	Extensive NLF runs measured	Waviness measured
$9\text{-}18\times10^6$	$C_d, C_p, u/u_e$	$(x/c)_t = 50\%$	No appreciable NLF on production surface Propeller slipstream effects measured
$7.7\text{-}19.7\times10^6$	$C_d, C_p, u/u_e$	$(x/c)_t = 20\%$ $C_{d_{min}} = 0062$	Waviness measured
$0.25 < M < 0.78$ $8.4\text{-}23.1\times10^6$	C_d, C_p	$C_{d_{min}} = 0.0097$ [compare to Eq. (17)]	No appreciable NLF on production surface Waviness and roughness measured
20×10^6	C_d, C_p	$(x/c)_t = 60\%$	Waviness measured
17×10^6	C_d, Sublimating chemicals	$(x/c)_t = 65\%$	Waviness measured No appreciable NLF on production surface
$M = 0.7$ 30.4×10^6	Sublimating chemicals, C_p	$(x/c)_t > 50\%$	Waviness measured
	C_d, sublimating and oxidizing chemicals, $C_p, u/u_e$		Waviness measured No appreciable NLF on production surfaces
17×10^6	C_d, sublimating chemicals	Skin joint filler cracks most serious surface maintenance problem	Insect contamination discussed Laminar flow maintainability studied
Up to 30×10^6	u/u_e	$(x/c)_t = 56\%$ at $G = 10$ deg	Sweep effects studied
$1.2 < M < 2$	Hot films, sublimating chemicals	$1.2 < R_t < 8\times10^6$	Less laminar flow on production than on gloved surfaces

gradients (accelerating flow) that limit the growth of two-dimensional disturbances [Tollmien-Schlichting (T-S) waves] in the boundary layer. On the other hand, the growth of T-S waves can be aggravated by the effects of surface waviness on local pressure gradients and boundary-layer velocity profiles; these effects reduce boundary-layer stability and can lead to premature transition. Thus, favorable pressure gradients "protect" the laminar boundary layer from the effects of limited amounts of surface waviness by counteracting the destabilizing influences of waviness. Similar influences govern the critical sizes of other two-dimensional protuberances such as steps and gaps in the laminar boundary layers. The maintenance of NLF on the wings requires that the surfaces be kept free in an operating environment from critical amounts of surface contamination (e.g., insect debris or ice), freestream disturbances (e.g., noise and turbulence), and surface damage. Compared to phenomena affecting the achievability of NLF, less is understood about maintainability of NLF under the wide ranges of Reynolds numbers, Mach numbers, meteorological conditions, flight profiles, and aircraft configurations that characterize the potential applications for NLF. It is generally true, however, that ease in maintenance of the NLF surface improves as the Reynolds number decreases. In summary, the critical issues concerning the practicality of NLF for drag reduction are twofold: 1) can practical production surfaces meet the roughness and waviness critical for achievement of NLF under high-speed conditions, and 2) can laminar flow benefits be cost effectively maintained in typical aircraft operating environments?

Past research has left a mixture of positive and negative conclusions concerning these questions. A significant consensus from early research (circa 1950) was that the airframe surface quality required for NLF could not be achieved in the metal airframe mass production methods of that time (see Ref. 1, Chap. 5). Close examination of those fabrication methods reveals the shortcomings to have been excessive waviness between the ribs and stringers, excessive step heights or gap widths at the skin joints, and excessive heights of protuberances from certain riveting techniques (press-countersunk or dimpled rivets, for example). Previous NLF flight experiments[2-26] in which the transition location and/or section drag were determined are summarized in Table 1. These experiments included both unprepared (production) surfaces and specially prepared (filled and sanded) surfaces and airfoil gloves. The experiments on the production quality surfaces[7,9,11,16,18,21,23,26] of that period resulted in little or no laminar flow due to the fabrication shortcomings noted above. However, on the specially prepared surfaces and on gloves (see Table 1), the transition locations and airfoil performance typically closely matched the theoretical predictions and low-turbulence wind-tunnel model test results. The successes of the prepared and gloved surface tests provided the initial guidance for the development of criteria for allowable waviness as well as for allowable two- and three-dimensional protuberance heights. Development of these criteria was also strongly based on wind-tunnel research. A summary of these criteria is presented in Ref. 27. In general, these criteria provide conservative guidance for the manufacture of NLF surfaces. This conservatism stems from their development origins in wind tunnels where "stream disturbances may exacerbate roughness problems."[28] In the past, the conservatism may have been partly responsible for the perception that NLF would be very difficult to achieve, even on modern production surfaces. This perception was probably heightened by the relatively high unit Reynolds number range, $R_c > 2\times10^6$ ft^{-1}, for the World War II high-performance fighters on which early NLF applications were attempted; such freestream conditions make the laminar boundary layer very sensitive to surface imperfections and insect contamination.

Even when the proper surface quality can be achieved, a concern that remains the subject of much research is the effect of operating environments on NLF maintainability. Past research has increased our understanding of some of the physical instability phenomena resulting from the exposure of laminar boundary layers to vibration, atmospheric particles (ice crystals), turbulence, and noise. Reference 28 summarizes much of this past work. The literature concludes that airframe vibration does not significantly influence laminar boundary-layer stability for many important practical applications.[27,29] The effects of atmospheric turbulence on laminar stability have been determined to be inconsequential.[2-4,8,28] Studies on the effects of atmospheric particles[27,28] have identified the potential for a significant loss of laminar flow on swept-wing laminar flow control airplanes during flight through high-altitude (stratospheric) ice crystal clouds. At lower altitudes, where liquid-phase cloud particles exist, little research has been done to determine the influence of such cloud particles on the laminar flow of either swept or unswept wings. Studies of the influence of noise on laminar stability have shown the potential for loss of laminar flow due to turbine engine noise impingement on laminar surfaces.[27,28] Limited evidence exists that engine/propeller noise on piston-driven airplanes may slightly affect the transition position on NLF surfaces.[10] The literature is not conclusive on the operational seriousness of insect contamination and propeller slipstream disturbances to the laminar flow.

In recent years, two major trends in airplane fabrication and operations have developed that are favorable to NLF. First, modern airframe construction materials and fabrication methods offer the potential for the production of aerodynamic surfaces without critical roughness and waviness. These modern techniques include composites, milled aluminum skins, and bonded aluminum skins, among others. The second modern trend favorable to NLF is the relatively lower range of Reynolds numbers for current high-performance business airplanes (see Fig. 1). Most of these airplanes cruise at unit Reynolds numbers of less than 1.5×10^6 ft^{-1}, making the achievement of NLF-compatible surface quality relatively easier. This trend results from larger wing loadings and aspect ratios that produce shorter chord lengths and from the much higher cruise altitudes possible for modern airplanes.

It is significant to note that NLF has been a practical reality for one category of aircraft—sailplanes. The achievement of laminar flow on sailplanes has been facilitated by the lower chord Reynolds numbers [Typically $R_c < 4\times10^6$ (see Fig. 1).] at which they operate, relative to most power airplanes, and by the use of composite construction methods to produce smooth complex shapes. Based on the successful NLF experience on sailplanes, the following question arises: what are the maximum Reynolds number, Mach number, and sweep angle ranges where the smoothness of modern, practical airframe construction techniques will fail to meet requirements for NLF in favorable pressure gradients?

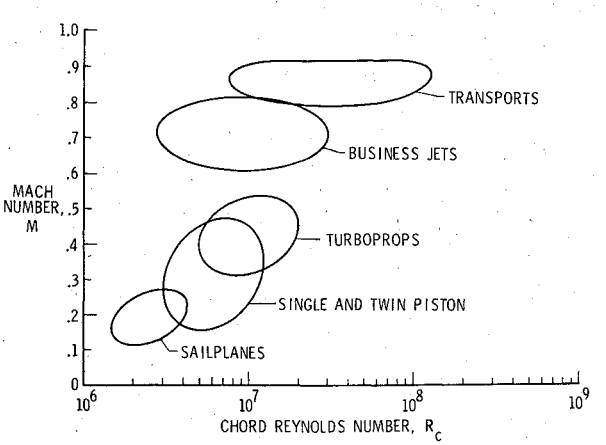

Fig. 1 Representative cruise Mach and Reynolds numbers for several airplane classes.

This paper presents the results of several NLF flight experiments conducted by NASA during the past 2 yr seeking to answer this question. These experiments were designed to address the issues of achievability of NLF on production-quality airframe surfaces and its maintainability in operating environments. The significant factor distinguishing these recent flight experiments from those of the 1930s and 1940s is the difference in preflight preparation of the surfaces tested. The recent experiments were conducted on "production-quality" surfaces, that is, on surfaces that received (with two noted exceptions) no modification by filling and sanding to meet the airfoil contour or waviness requirements for NLF. This paper presents the major results of these flight experiments and the implications of these results for airplane design, flight test procedures, and further studies.

Flight Experiments

In the past year, NLF flight experiments[30,31] were conducted on eight different airplanes of the (seven) types listed in Table 2 and shown in Fig. 2. The general objective of these flight experiments was to investigate the extent of NLF and the factors affecting transition to turbulence on a wide variety of modern, production-quality smooth airframe surfaces tested under various operating conditions. The airplanes chosen for the experiments had relatively stiff skins, free from significant roughness and waviness, and possessed relatively long runs of proverse pressure gradients, favorable to laminar boundary-layer stability. The methods of airframe construction for the test airplanes are given in Table 2. A ninth airplane, not listed in Table 2, is the T-34C that was used for studying the effects of a propeller slipstream on the laminar boundary layer.

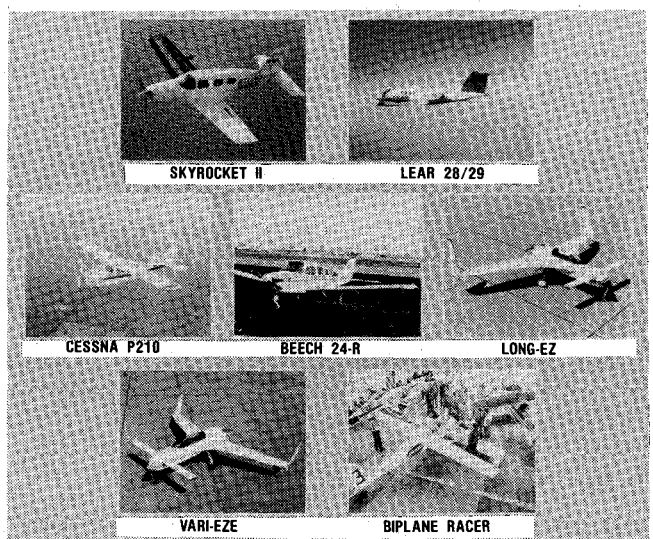

Fig. 2 Airplanes selected for NLF flight experiments.

Most of the surfaces evaluated for laminar flow received no special surface contour preparation prior to testing. However, in two of the tests (Cessna 210 and Learjet 28/29), the leading-edge butt joints or rivet rows were faired over to eliminate gross disturbances to the boundary layer. For the remaining six airplanes, the standard production-quality surfaces were tested. In the case of Skyrocket II, the airplane had been unprotected from the natural environment at the Charleston, W. Va., airport where it was parked outside for over 5 yr. Prior to testing, the airplane was painted, but no smoothing of the airfoil contours was performed. The significant point in common for all of the airplanes tested was that they possessed low levels of surface waviness and roughness, which are currently achievable in production and which appear maintainable over extended periods of airframe life.

Specific objectives of the experiments included measurements or observations of the following:

1) Boundary-layer, laminar-to-turbulent transition locations on a variety of aerodynamic surfaces including swept and unswept wings, fuselage nose, wheel fairing, horizontal and vertical stabilizers, and propeller spinner and blade airfoil surfaces.

2) Effect of the nearly total loss of laminar flow (fixed transition at 5% chord) on airplane performance, stability, and control.

3) Effect of propeller slipstream on wing boundary-layer transition and on boundary-layer profiles.

4) Wing section profile drag.

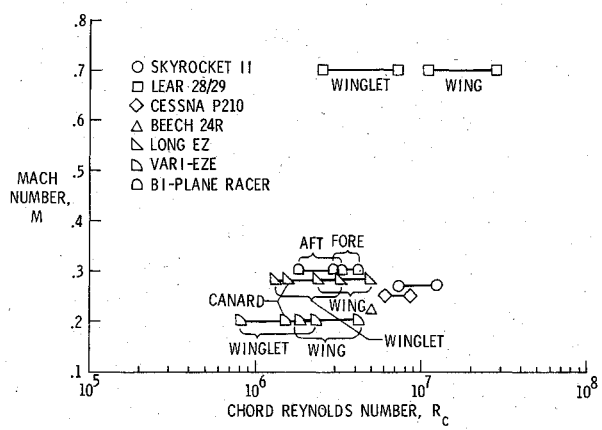

Fig. 3 Freestream conditions for NLF flight experiments.

Table 2 Airplanes used in natural laminar flow (NLF) flight experiments

Airplane	Construction	Surface	c, ft	Λ, deg	Airfoil
Bellanca Skyrocket II	Fiberglass/aluminum honeycomb	Wing	5.37	3	NACA 63_2-215
Gates Learjet Model 28/29	Milled aluminum skins, integrally stiffened[a]	Wing	6.92	17	NACA 6 series
		Winglet	1.73	40	LS(1)-0413 mod.
Cessna P-210	Dimpled, flush-riveted aluminum[b]	Wing	5.08	0	NACA 64 series
Beechcraft Model 24R	Bonded aluminum skins/honeycomb ribs	Wing	0	0	63_2A-415
		Propeller	0.54	—	Clark Y
Rutan Long-EZ[c]	Fiberglass/foam core	Wing	3.13	23	Eppler
		Winglet	1.71	28	Eppler
		Canard	1.08	0	GU25-5(11)8
Rutan VariEze	Fiberglass/foam core	Wing	2.58	27	LS(1)-0417 mod.
		Winglet	1.21	29	LS(1)-0417 mod.
		Canard	1.08	0	GU25-5(11)8
Rutan Biplane Racer	Fiberglass or graphite/foam core	Fore wing	2.67	6	Eppler
		Aft wing	1.92	3	Eppler

[a] Leading edge to skin butt joint filled and faired smooth.
[b] Portion of test section filled and faired smooth.
[c] Two different Long-EZ airplanes were tested to confirm consistency of transition results.

5) Effect of flight through clouds on boundary-layer transition.

6) Insect debris contamination effects.

The test conditions for the experiments are shown in Fig. 3. Because of the variety of geometric shapes existing on each of the aircraft (tapered wings, for example) and the range of operating flight speeds and altitudes, ranges of Reynolds numbers, based on local chords, are given for individual airplane components.

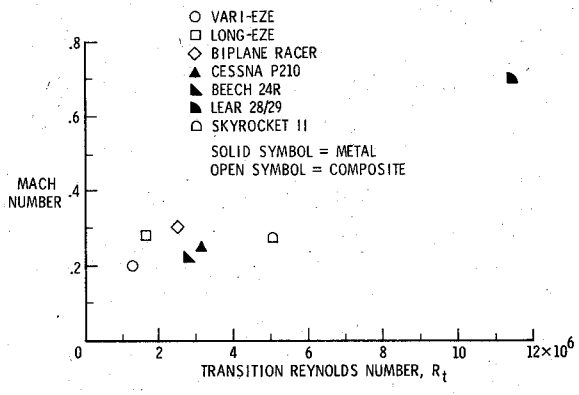

Fig. 4 NLF transition Reynolds numbers from flight experiments.

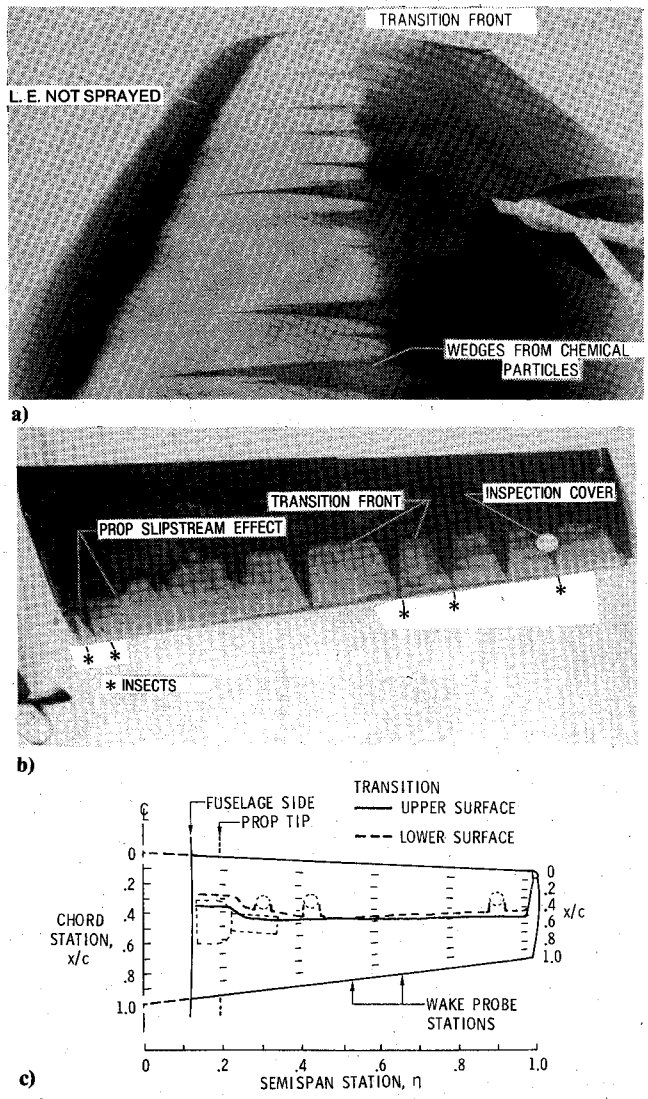

Fig. 5 Bellanca Skyrocket II flight data: a) upper surface transition, b) lower surface transition, and c) nondimensional transition locations.

Experimental Methods

For all of the airplanes tested, boundary-layer transition location measurements were made using the sublimating chemical technique.[32-34] The technique involves coating the surface with a thin film of a volatile chemical solid that, during exposure to freestream airflow, rapidly sublimates in the turbulent boundary layer due to heat transfer. The chemical coating remains relatively unaffected in the laminar region because of the lower heat-transfer rates, thus indicating transition. The use of a chemical such as acenaphthene at ambient temperatures between 30 and 90°F offers the capability to fly to low-altitude test points (<20,000 ft), stabilize the sublimating chemical pattern at the desired test conditions, and return to the ground with the chemical pattern unaffected by the off-condition portions of the flight. The resulting range of flight times at the test conditions vary between about 60 and 5 min, respectively, for the temperatures given. Further details on the use of the technique are given in Ref. 31.

Flight measurements on the Skyrocket II airplane included wake profiles using a wake rake for section profile drag determination, boundary-layer profiles measured using boundary-layer rakes, and section lift coefficients determined using pressure belt measurements. Speed-power data were recorded to determine relative airplane drag polar changes from free to fixed transition. For tests on the airplanes that included fixed transition, thin grit strips (1/8 in. wide) with grit sized by Ref. 35 were located at $x/c=5\%$ on upper and lower component surfaces. Measurements of the time-dependent nature of the laminar boundary layer immersed in a propeller slipstream were made using glue-on hot-film transition detectors on the T-34C airplane. These hot films were also used to observe the effect of flight through clouds on laminar flow.

Laminar Flow Observations

Transition Locations

The location of boundary-layer transition on the lifting surfaces evaluated was observed generally to occur downstream of the analytically estimated minimum pressure locations for each airfoil at its particular flight conditions. Thus, transition is caused either by amplification of two-dimensional T-S instabilities in the adverse pressure gradient regions or by laminar separation. The transition Reynolds numbers for the largest chords on each of the various components tested on each airplane are shown in Fig. 4. Transition Reynolds numbers were $1\text{-}5\times10^6$ for the propeller-driven airplanes, and exceeded 11×10^6 for the business jet tested. Examples of boundary-layer transition visualization by sublimating chemicals are shown in Fig. 5.

Figure 5a illustrates the transition locations on the upper and lower wing surfaces at a unit Reynolds number of 1.884×10^6 ft^{-1}. Airplane trimmed lift coefficient was 0.22 at $M=0.31$. The turbulent wedges seen in Fig. 5a were caused by large chemical particles that adhered to the surface during application of the coating. Turbulent wedges caused by insects on the lower surface are marked with an asterisk in Fig. 5b; the unmarked wedges were caused by artificial trips (grit). Note the absence of any chemical particle-induced wedges in this pattern; this resulted from mechanically loosening the particles by brushing the chemical coating prior to flight. The measured nondimensionalized transition positions are summarized in Fig. 5c.

Figure 6 shows the agreement between measured and predicted[36] pressure distributions for the actual Skyrocket airfoil contour at the pressure belt station on the left wing. The agreement illustrates the satisfactory accuracy of using the measured contours to predict pressure distributions. The predicted transition locations at the wake probe stations on the right wing are shown in Fig. 7 along with flight-measured transition locations. The theory predicts transition slightly

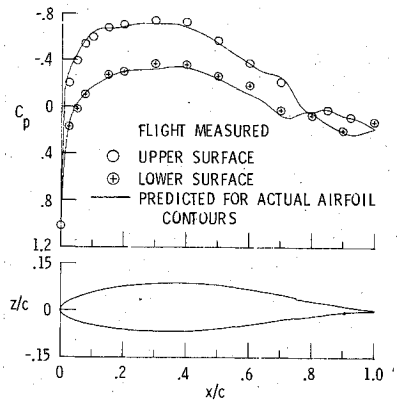

Fig. 6 Skyrocket wing: predicted and flight-measured pressure distributions (left wing) ($R_c = 8.8 \times 10^6$, $C_l = 0.288$, $M = 0.31$).

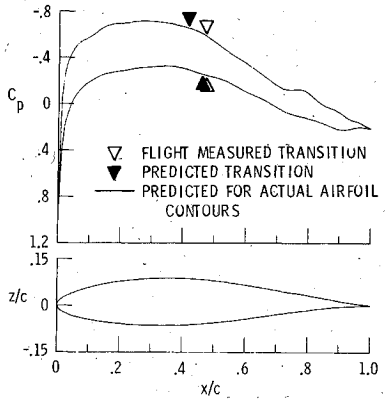

Fig. 7 Skyrocket wing: flight-measured and predicted transition locations (right wing), inboard wake probe station ($R_c = 9.04 \times 10^6$, $C_l = 0.288$, $M = 0.31$).

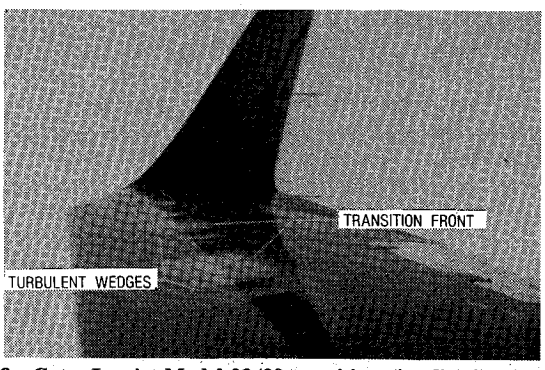

Fig. 8 Gates Learjet Model 28/29 transition visualization ($M = 0.7$, $R_x = 3.08 \times 10^6$ ft^{-1}, $C_L = 0.12$).

ahead of the flight-measured locations (but still in the region of adverse pressure gradient). This might be explained as a result of the use in Ref. 36 of the Granville curve to predict transition based on an empirical correlation with boundary-layer characteristics at the points of laminar instability and transition. This correlation was developed using low-turbulence wind-tunnel data; thus, in flights with even less freestream turbulence, the criterion may be slightly conservative. The fact that transition with chemicals on the wing occurs further downstream than both the analytically predicted transition locations (with no accounting for chemical "roughness") and the point of minimum pressure provides confidence that chemicals can be used without concern (at these test conditions) for any chemical-induced effects on transition location.

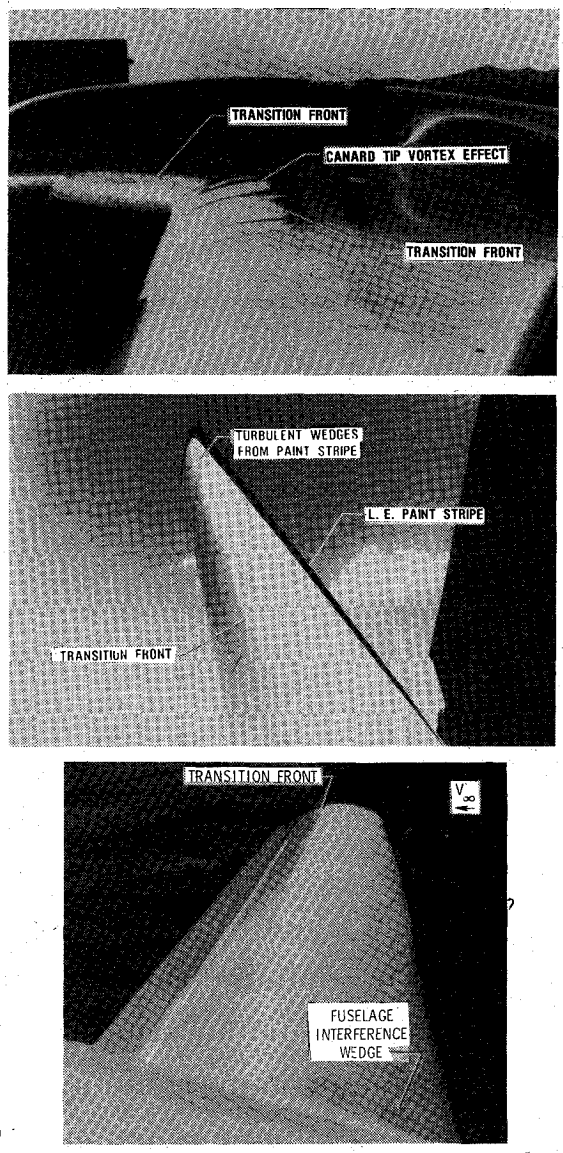

Fig. 9 Boundary-layer transition visualization on the Rutan Long-EZ ($R_x = 1.42 \times 10^6$ ft^{-1}, $C_L = 0.16$): a) wing and strake, b) winglet, and c) canard.

Transition on the upper surface of the Learjet wing (Fig. 8) was located near $(x/c)_t = 40\%$ across the span for $M = 0.7$, $R_{\bar{c}} = 21.7 \times 10^6$, and $C_l = 0.2$. Free transition on the inboard side of the winglet was observed to occur as far back as $(x/c)_t = 55\%$. The unit Reynolds number during this test was $R_x = 3.08 \times 10^6$ ft^{-1}. This large value of R_x resulted from the low-density altitude (16,500 ft) selected to facilitate the use of sublimating chemicals in the winter. A normal cruise unit Reynolds number for this airplane would be $R_x = 0.87 \times 10^6$ ft^{-1} for $M = 0.76$ at 51,000 ft cruise. Thus, the transition data from the Learjet tests were gathered at a higher Reynolds number than is required during normal operations.

Boundary-layer transition locations on the wing and strake, winglet, and canard of the Rutan Long-EZ are shown in Fig. 9 for $R_x = 1.42 \times 10^6$ ft^{-1} and $C_L = 0.16$. Wing upper surface transition is shown in Fig. 9a located at $(x/c)_t = 32\%$ along the wing span. For the wing airfoil at the test conditions, proverse pressure gradients were estimated theoretically to exist to about $(x/c)_{\text{u.s.}} = 30\%$. On the strake, transition occurs (Fig. 9a) near $(x/c)_t = 10\text{-}15\%$. Transition on the winglets of this airplane (Fig. 9b) was observed at $(x/c)_t = 32\%$ on the inboard suction side and at $(x/c)_t = 55\%$ on the canard upper surface (Fig. 9c).

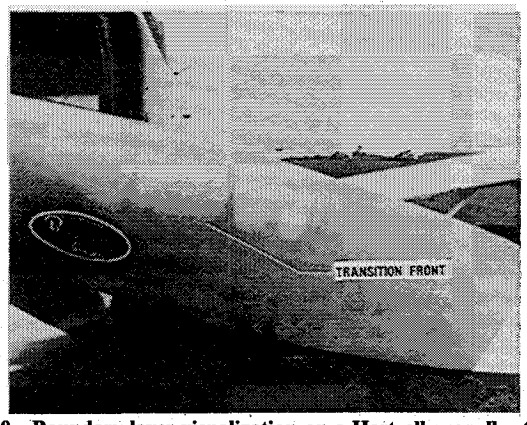

Fig. 10 Boundary-layer visualization on a Hartzell propeller (Beech Model 24R airplane) ($V = 140$ knots, $n = 2700$ rpm).

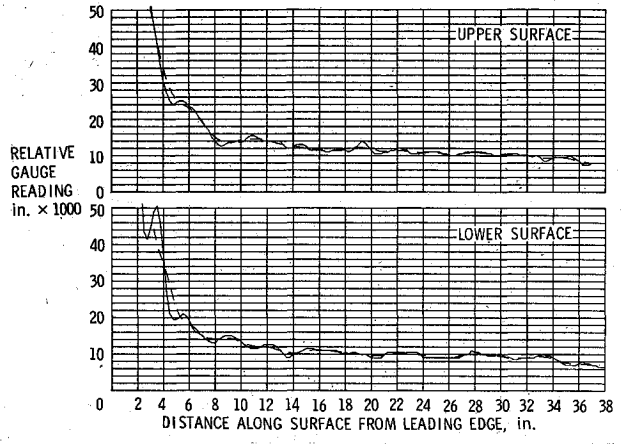

Fig. 11 Indicated surface waviness for the Bellanca Skyrocket II at the inboard wake probe station.

Figure 10 illustrates laminar flow on the propeller of the Beech Model 24R airplane. Boundary-layer transition was seen at $(x/c)_t = 38\%$ on the forward (suction) side and at $(x/c)_t = 80\%$ on the aft (pressure) side of the blade. The test was conducted at $V = 133$ knots, 2700 rpm, and $J = 0.84$. These conditions produce a local unit Reynolds number on the blade at the 50% blade radius location of $R_x = 2.89 \times 10^6$ ft^{-1} and a local Mach number of 0.46.

Transition location observations on the remaining airplanes listed in Table 2, but not discussed here, were of the same nature as above. That is, the laminar flow extended typically to positions slightly beyond the predicted or estimated location of minimum pressure.

Surface Conditions and Contours

No premature transition that could be attributed specifically to surface waviness was observed in any of the tests. Surface waviness measurements* were made for all but two of the airplanes tested. An example of waviness is given in Fig. 11 for the Skyrocket II. The difference between the solid and the dashed lines serves to indicate wave height. The largest indicated wave height appears near the leading edge of the lower surface where $h \simeq 0.015$ in. near $s = 4$ in., $(x/c) = 6.5\%$. This particular wave occurred at the bonded leading-edge attachment joint. More typical wave heights were about $h = 0.002$ in.

*Surface waviness was measured with a dial indicator on a 2 in. base and is referred to as indicated waviness since the recorded values of wave amplitude and wave numbers are magnified to some extent by the measuring device.[27]

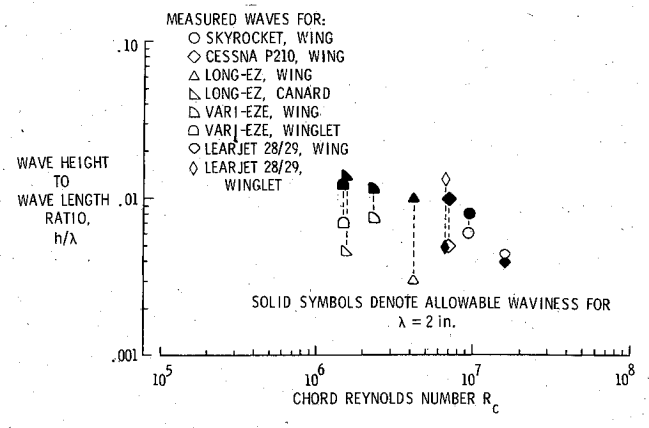

Fig. 12 Comparisons of allowable and actual waviness for NLF flight experiment data.

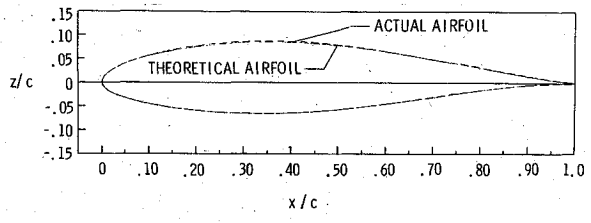

Fig. 13 Comparison of the NACA 63_2-215 and actual airfoil contours for the Bellanca Skyrocket II (inboard wake probe station).

Conservative agreement exists between the allowable and indicated wave heights for all of the surfaces tested, where allowable wave heights were estimated using the criterion from Ref. 27,

$$\frac{h}{\lambda} = \left(\frac{59{,}000\, c \cos^2 \Lambda}{\lambda R_c^{1.5}}\right)^{1/2} \tag{1}$$

For multiple waves, h/λ is one-third the value for a single wave.

The differences between indicated and allowable waviness for selected measurement locations on the airplanes tested for NLF are shown in Fig. 12. The allowable waviness (h/λ) is determined from Eq. (1) for the chord length at the largest wave found and for the flight Reynolds number. As shown in the figure, for the surfaces tested, only one wave existed that exceeded the empirical criterion. The exception for the Lear 28/29 winglet occurred due to an aft-facing skin lap-joint step that caused premature transition. Although this step is not actually a wave, it was measured and recorded as a wave in the figure for correlation with the criterion. Since the testing was conducted at low altitudes and high speeds, the allowable waviness at more typical cruise conditions for each airplane will be somewhat larger.

On the Skyrocket, measurements were made of airfoil contours existing on the wing tested. Figure 13 illustrates the comparison at one wing station between theoretical NACA 63_2-215 and actual section shapes. Deviations between the actual and theoretical contours as large as 0.117 in. were measured on the upper surface. Calculations (using Ref. 36) of the airfoil pressure distribution and transition characteristics predict small effects for the contour deviations measured as shown in Fig. 7 by comparing the data for the theoretical and actual airfoils. The waviness and contour measurements and analyses discussed here are evidence of the ability, with modern airframe manufacturing methods, to produce surface conditions that can conservatively meet NLF roughness and waviness requirements.

Profile Drag and Fixed-Transition Effects

While the determination of transition locations is significant to the understanding of airplane performance, it is the measurement of lifting-surface profile drag, correlated with transition locations, that provides a complete understanding of airframe performance. It is also important to understand the effects on airplane aerodynamics that can occur due to the total loss of laminar flow (fixed leading-edge transition).

Flight-measured wing profile drag for the Bellanca Skyrocket II at the inboard wake probe station (see Fig. 5c) is presented in Fig. 14 for free and fixed transitions. This figure also presents the wind tunnel-measured characteristics for the NACA 63_2-215 airfoil with free transition and the predicted[36] drag polars for the measured airfoil contour. As shown, excellent agreement exists between the tunnel[37] and flight experiment drag polars. With fixed transition for cruise lift coefficients ($C_l < 0.3$), the wing section profile drag increases by 80%. With transition fixed on both the wing and empennage surfaces at 5%, total airplane drag at cruise (based on the power required at a given speed) increased 23%. The benefit of laminar flow on the cruise range performance of this airplane was calculated using a parabolic drag polar assumption for the airplane, the airplane zero lift-drag coefficient with laminar flow-of 0.0163 (from Ref. 38), Oswald's airplane-induced drag efficiency factor of 0.80, a constant value of brake specific fuel consumption of 0.56, and a propulsive efficiency of 0.85. At the same speed, the drag reduction with laminar flow on the Skyrocket increases cruise range by 25% (with constant Breguet factor).

For one of the Rutan Long-EZ airplanes tested,[30] the effects of fixed transition on airplane performance and longitudinal trim characteristics are presented in Fig. 15. This configuration experienced an 11 knot increase in minimum trim speed, corresponding to a 27% decrease in trimmed maximum lift coefficient. Maximum speed for the airplane was reduced with fixed transition by 11 knots, corresponding to a 24% increase in cruise drag. Figure 15 illustrates a large increase in trim elevator deflections with fixed transition on the airplane. In addition to the preceding performance degradation, qualitative observations were made of a reduction in short-period damping at cruise speeds. Wind-tunnel experiments[30] confirmed that on the 20% thick NLF canard airfoil, fixing transition near the leading edge caused extensive separation of the thickened turbulent boundary layer near the trailing edge over the elevator. Similar large changes in performance and longitudinal stability and control were observed for one of the other airplanes tested, the Rutan VariEze.[30] The effects of fixed transition on this airplane included a reduction in trimmed airplane lift curve slope of about 7%, and a reduction in the lift curve slope of the canard of about 30%. These effects are not a consequence of canard configurations but rather due to the characteristics of the airfoil selected for the canard surface. By conservative NLF airfoil design, these effects can be entirely avoided.

Such large effects of the loss of laminar flow on the airplane aerodynamic characteristics indicate the importance of fixed-transition flight testing as a standard procedure for any airplane that possesses long runs of proverse pressure gradient and smooth aerodynamic surfaces capable of supporting NLF. In addition, free-transition flight testing methods should account for transition locations across all aerodynamic surfaces, using sublimating chemicals or another cost-effective technique.

Propeller Slipstream Effects

Past observations of the effect of the propeller slipstream on boundary-layer transition,[5,6,16,17,29,37,39] produced varying conclusions. The research reported by Young[5,6] and Hood[29] concluded that the effect of the slipstream was to effectively move transition to the wing leading edge behind the propeller. In the case of Young's flight experiments, boundary-layer thickness, measured by a total pressure survey probe, was used to judge the transition location; where the measured boundary-layer thickness exceeded the calculated laminar thickness, transition was assumed to have occurred. Young thus reported transition near the leading edge on two different airplanes. Using similar methods, Hood reported similar results in wind-tunnel tests for a propeller-mounted 20% chord in front of the wing leading edge. Concerns about the validity of these conclusions are discussed below.

Experiments reported by Zalovcik[16,17] and Wenzinger[39] gave evidence that the effect of the propeller slipstream might not be as detrimental as in Young's and Hood's tests. Wenzinger's tunnel experiments showed moderate effects of propeller slipstream on section drag measured by a wake probe for an NACA 66 series NLF airfoil. Zalovcik reported extensive laminar flow in the propeller slipstream during his

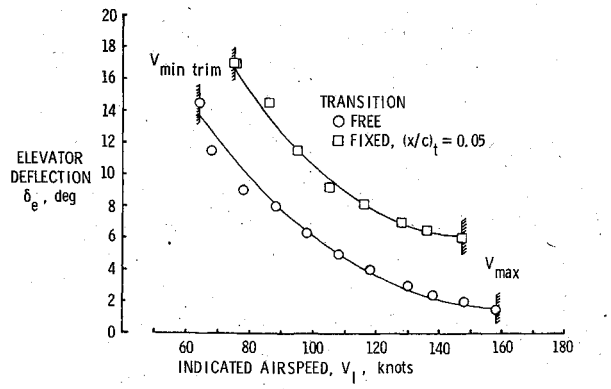

Fig. 15 Comparison of fixed- vs free-transition performance and longitudinal control characteristics for a Rutan Long-EZ in flight.

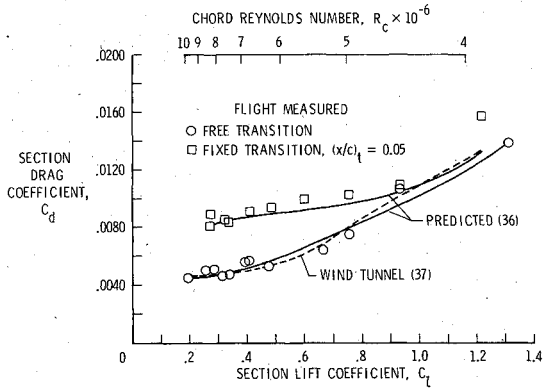

Fig. 14 Comparison of flight and wind-tunnel section characteristics for the Skyrocket II airfoil (inboard wake probe station).

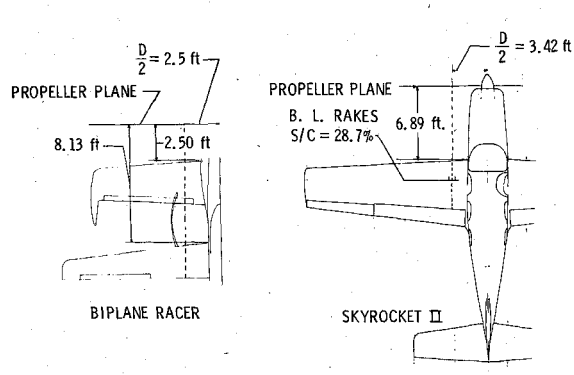

Fig. 16 Planviews of configurations used to study the effects of propeller slipstream on NLF.

flight experiments on the P-47 and P-51 airplanes. These latter flight experiments were the first to rely on detailed boundary-layer rake measurements to determine transition locations as indicated by large profile changes at transition.

Two of the recent flight experiments included observations and measurements of the laminar boundary layer in the slipstream on the configurations illustrated in Fig. 16. On the Rutan biplane racer[30] on the inboard portion of the aft wing immersed in the slipstream (see Fig. 17), the chemical pattern in the propeller slipstream was similar to that outside the slipstream, indicating transition at $(x/c)_t = 61\%$.

During the Skyrocket experiments that followed, more detailed measurements were made in the propeller slipstream. Figures 5b and 5c show that transition, as indicated by the chemical pattern, moved forward on the lower surface from $(x/c)_t = 40\%$ outside the slipstream to $(x/c)_t = 28\%$ inside. On the upper surface transition moved forward by a similar increment. An interesting detail was the lack of any apparent effect of the propeller tip vortices on transition where they impinged on the wing. One possible explanation for the forward motion of the chemical-indicated transition in the propeller wake is the effect of an increased disturbance environment in the propeller slipstream. These larger disturbances might amplify to transition earlier along the chord than the smaller disturbances outside the slipstream.

Time-averaged boundary-layer profiles were measured by rakes inside and outside the propeller slipstream with both free and fixed transitions on the Skyrocket (see Fig. 18). These measurements were made at $s/c = 28.7\%$, $R_x = 1.715 \times 10^6$ ft^{-1}, $M = 0.31$, and $n = 1800$ rpm. Inside the slipstream the estimated unit Reynolds number was 1.778×10^6 ft^{-1} (using propeller momentum theory).

With free transition, Fig. 18 shows the thin laminar boundary layer outside the propeller slipstream where $\delta \simeq 0.06$ in.; inside, the profile has thickened to $\delta \simeq 0.24$ in. and the profile has changed, appearing more turbulent in shape. This rake was positioned in the slipstream at a chordwise position that was laminar as shown by sublimating chemical patterns. Thus, this thickened profile was not a turbulent one in the normal sense. To verify the shape and thickness of an actual turbulent profile at this position, transition was fixed in front of the rakes inside and outside the propeller slipstream. The resulting turbulent profiles are seen in Fig. 18 as the solid symbols. It is apparent that the effect of the propeller slipstream on time-averaged boundary-layer profile measurements is to create a shape that is turbulent in appearance and that is increased in thickness to near the actual turbulent boundary-layer thickness ($\delta \simeq 0.28$ in. for the solid symbols).

The early measurements by both Young and Hood, using boundary-layer thickness or profile shape as an indication of transition, thus may have produced misleading conclusions about the effect of propeller slipstream on laminar flow. If this is true, then there may be no data in the literature properly concluding that propeller slipstreams cause premature transition.

A proposed explanation was offered in Ref. 40 for the "turbulent-appearing" time-averaged boundary-layer profile in the laminar region of the propeller slipstream. It was hypothesized that the cyclic impingement on the boundary layer of the propeller blade trailing-edge turbulent wake (vortex sheet) was received by the boundary layer as relatively small (chordwise) regions of transition that moved downstream in a coherent fashion. Then, between these turbulent packets, the boundary layer might be "normally" laminar. In time-averaged measurements, these locally cyclic transition regions might affect the profiles as shown in Fig. 18. Recently at NASA Langley, experiments were conducted using surface hot films in a laminar boundary layer in the propeller slipstream in flight on a T-34C airplane. These experiments confirmed the general validity of the proposed cyclic laminar boundary layer as shown in Fig. 19. However, this figure illustrates the true nature of this cyclic behavior. It can be seen that the sensor on the miniglove at the leading edge records a small laminar velocity rise disturbance at the propeller blade passing frequency. When this disturbance reaches the second, third, and fourth sensors, it has progressively grown in amplitude and in duration. The sensors on the NLF glove outside the propeller slipstream show the relative magnitudes of laminar and turbulent signals.

Such cyclic laminar behavior raises the question of the possibility of laminar flow drag reduction benefits on surfaces immersed in propeller slipstreams (i.e., wings, nacelles, and empennages). Analysis of Wenzinger's data[39] presented in Ref. 31 indicates that the drag increase of laminar airfoils in propeller slipstreams is significantly less than that due to total loss on laminar flow.

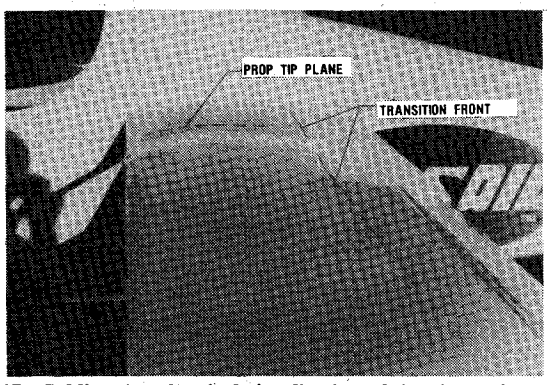

Fig. 17 Sublimating chemical visualization of the effect of propeller slipstream on transition on the Rutan Biplane Racer ($R_x = 1.38 \times 10^6$ ft^{-1}, $C_L = 0.13$, $n = 2700$ rpm).

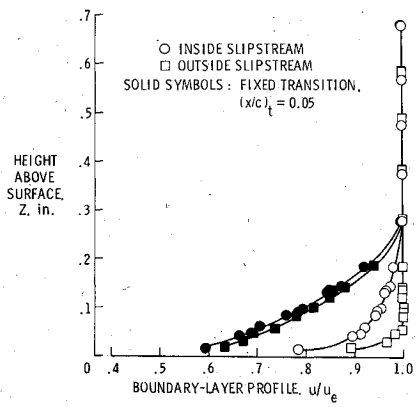

Fig. 18 Effect of propeller slipstream on Skyrocket II boundary-layer profiles ($s/c = 28.7\%$, $n = 1800$ rpm, $C_L = 0.21$).

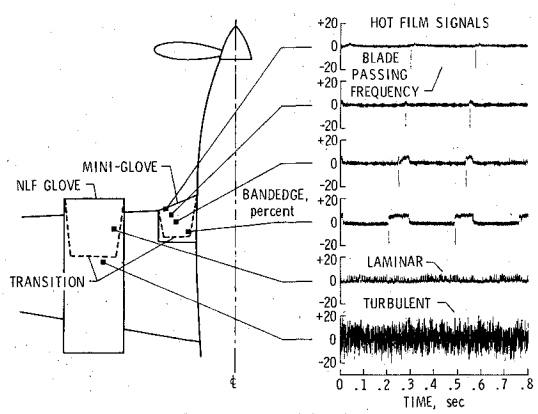

Fig. 19 In-flight, hot-film measured, time-dependent effects of propeller slipstream on the laminar boundary layer (T34C airplane).

A complete understanding of the phenomena involved in laminar boundary layers immersed in propeller slipstreams will be useful in developing methods to predict transition and possibly reduce section drag in these regions. It appears possible that significant levels of laminar flow drag reduction may be realized in propeller slipstreams.

Sweep Effects

The two significant phenomena related to wing geometry that can adversely affect laminar boundary layers on swept surfaces are cross-flow instability and turbulent contamination of the leading-edge attachment line flow (or leading-edge contamination). The analysis of the present NLF flight data has not yet included detailed analytical stability analysis. Since no obvious cross-flow instability was observed on the swept wings and winglets in the recent flight experiments, this discussion will center on leading-edge contamination.

A comparison between the recent flight data and the spanwise contamination criterion is presented in Fig. 20 for the VariEze and the Long-EZ.[30] The spanwise contamination criterion is summarized in Ref. 41 as

$$R_\theta = 0.404(\sin\Lambda/\sqrt{\cos\Lambda})\sqrt{R_x r_{\text{l.e.}}/(1+t/c)} \qquad (2)$$

where no spanwise contamination occurs for $R_\theta < 100$ and, depending on the surface conditions (roughness), there may be no spanwise contamination for $R_\theta < 240$. For $R_\theta > 240$, turbulent contamination from any source will freely propagate spanwise along the attachment line. On the swept main wings for both the VariEze ($\Lambda = 27$ deg) and the Long-EZ ($\Lambda = 23$ deg), the data in Fig. 20 show that $R_\theta = 100$ has not been exceeded. The same was true for the winglets on both airplanes where $R_\theta < 45$ for the VariEze and $R_\theta < 36$ for the Long-EZ. On the swept strakes of both the VariEze ($\Lambda = 61$ deg) and the Long-EZ ($\Lambda = 51$ deg), R_θ exceeded 100; still, small regions of laminar flow were observed near the leading edges of both strakes. Perhaps the smoothness of the leading edges permitted laminar flow with $R_\theta > 100$. Alternately, relaminarization might have been responsible for the short laminar runs observed in the strakes. On the Long-EZ, on the very short inboard strake ($\Lambda = 64$ deg) where $R_\theta \simeq 240$, no laminar flow was recorded by the chemical pattern. At the leading-edge break between $\Lambda = 64$ and 51 deg, the leading-edge contamination from the 64 deg swept region was not observed to propagate onto the 51 deg swept region in spite of $148 < R_\theta < 127$ for this region (see Fig. 17b).

On the Learjet wing ($\Lambda = 17$ deg), $R_\theta = 100$ was not exceeded in spite of the extremely high unit Reynolds number during the test.[30] On the Learjet winglet, where R_θ varied from 151 at the root to 75 at the tip during the tests, it could not be ascertained whether or not spanwise contamination was present on the portions of the winglet that were turbulent. This uncertainty was due to excessive roughness in the form of screw heads and a step that caused transition in some regions of the leading edge.

Even if spanwise contamination was present at the test condition where $R_x = 3.08 \times 10^6$ ft^{-1}, at typical cruise where $R_x = 0.87 \times 10^6$ ft^{-1}, the values of R_θ would drop to 80 at the winglet root and 40 at the tip, thus insuring no spanwise contamination. In fact, at the Learjet cruise unit Reynolds number given above, on a surface swept 40 deg, the leading-edge radius could be as large as 1.5 in. and still keep $R_\theta < 100$ for no spanwise contamination.

This observation implies that, in general, on certain relatively large lifting surfaces, spanwise contamination at high-altitude cruise may not be a serious concern. On the Gulfstream American GIII airplane, for example (chosen for its large size in the business jet class), at 45,000 ft and $M = 0.85$ cruise, R_θ varies from 80 at the wing root to 68 at the tip, precluding spanwise contamination. As a final example of operations below the spanwise contamination criterion, R_θ for the DC-10 winglet[42] varies from 64 at the root to 40 at the tip for $M = 0.82$, 35,000 ft cruise. At a cruise unit Reynolds number of about 1.9×10^6 ft^{-1}, the waviness requirements for a DC-10 winglet surface appear attainable.

Based on these observations, it appears that for certain important potential applications, spanwise contamination need not be a concern for relatively large lifting surfaces. Of course, the final design of a swept NLF surface will also be strongly influenced by cross-flow stability considerations.

Flight Through Clouds

The effects of flight through liquid-phase clouds on laminar flow was observed using the surface-mounted hot-film transition detectors on the T-34C airplane with a natural laminar flow glove. These flights were conducted at a true airspeed of 166 knots at density altitudes between 5000 and 7000 ft; these conditions yield a unit Reynolds number of about 1.5×10^6 ft^{-1}. During the transits in and out of clouds, the hot-film signals were observed using an onboard oscilloscope. During flight inside clouds for which no deposit

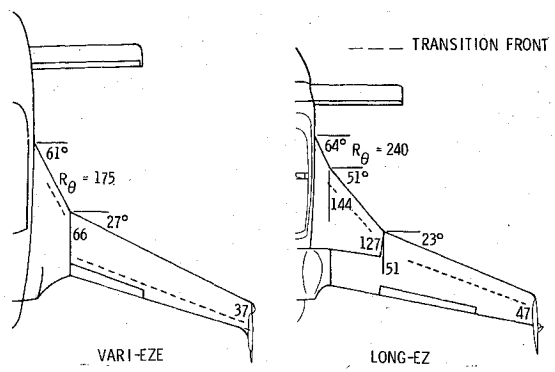

Fig. 20 Comparison of NLF flight data on swept surfaces with the spanwise contamination criterion.

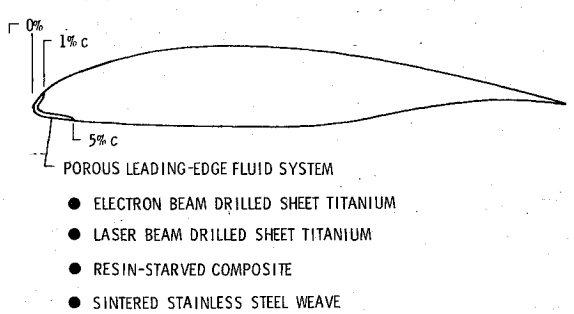

Fig. 21 Ice and insect contamination protection system concept for NLF wings.

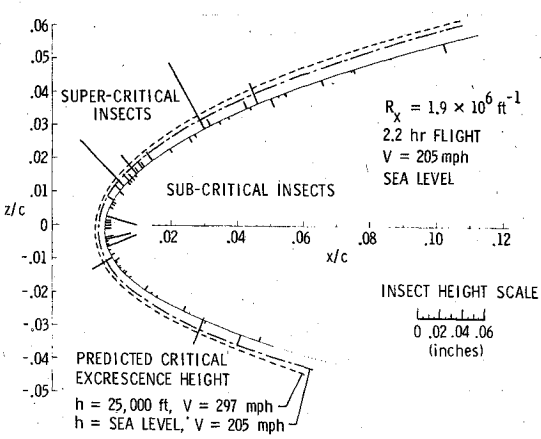

Fig. 22 Insect contamination pattern on the Skyrocket II NLF wing, accumulated in flight.

of mist on the windscreen nor laminar glove occurred, the boundary layer remained laminar to near the 40% chord station (the same transition location as for flight in clear air). When mist was observed to accumulate on the canopy windscreen and on the glove leading edge in clouds, the hot films indicated turbulent boundary-layer conditions at all chordwise stations from the leading edge to the 40% chord hot-film locations. Upon exiting the cloud, the boundary layer quickly reverted to the laminar state. These results indicate that laminar flow may not be lost during flight through certain combinations of cloud particle and unit Reynolds number conditions; further understanding of the conditions required for laminar flow loss on both swept and unswept wings is needed.

Insect Debris Contamination

The effect of contamination of NLF wings by insect debris is an important consideration in NLF airfoil design as well as in the operation of airplanes with laminar flow wings. These considerations, as well as insect population characteristics, are discussed in some detail in the literature.[43-49] In practice, the seriousness of insect debris contamination will likely be dependent on the airplane mission characteristics. On business airplanes, for example, it may be reasonable to expect an airplane operator to wipe the wing leading edge clean as part of the normal walk-around preflight inspection. In an intensive utilization mission, as with commuter airliners, ground turnaround times may not allow for leading-edge cleaning between frequent landings. Also, for very large airplanes, preflight cleaning of leading edges appears impractical. In these latter cases, active methods of insect protection such as porous, fluid-exuding leading edges may serve the purposes of both insect and ice protection (see Fig. 21). The ice protection performance features of such systems are discussed in Ref. 50, and the ability of wetted leading edges to protect against insect debris contamination is discussed in Refs. 51 and 52.

During the Skyrocket tests, a 2.2 h flight was conducted at less than 500 ft above ground level at $V_c = 176$ knots to collect a sample insect debris contamination pattern and to distinguish by chemical sublimation between which insect strikes caused transition (supercritical) and which did not (subcritical). This flight was conducted in late March after several weeks of warm weather in the Tidewater region of Virginia between 1430 and 1630 Eastern standard time. Figure 22 depicts the heights and positions of the insects collected along the span of the right wing and Fig. 5b shows the lower surface insect debris contamination wedges for this flight.

As illustrated by Fig. 22, only about one-fourth of the insects collected were of supercritical height at their chordwise locations and caused transition. Very near the stagnation point, rather large insect remains were recorded that did not cause transition. The long duration of the flight and the relatively rapid response of the chemicals to boundary-layer turbulence, especially on the forward part of the airfoil, make it unlikely that any supercritical insect strikes occurred which did not record a transition wedge in the chemical pattern. For the 3 deg wing washout, the stagnation line on this leading edge varied approximately $0 < (x/c) < 0.2\%$ at the test conditions.

The supercritical insect strikes shown are conservative in that the unit Reynolds number during the sea level test ($R_x = 1.9 \times 10^6$ ft^{-1}) was about 25% greater than a typical 25,000 ft cruise value ($R_x = 1.4 \times 10^6$ ft^{-1}). Thus, many of the insects that were supercritical at low altitudes would become subcritical at cruise altitudes. This fact is demonstrated by the boundaries drawn on Fig. 22 for critical roughness height at sea level and at 25,000 ft. These boundaries of critical three-dimensional roughness height were calculated by the method of Ref. 35. At the high-altitude cruise condition, only six insects or about 9% of the total insects collected, would cause transition. This trend of increased critical roughness height results from the smaller unit Reynolds numbers at higher altitudes.

The sample insect contamination data presented here serve to illustrate a certain inherent level of insensitivity of this particular combination of airfoil geometry and operating conditions to insect contamination. Examples of varying sensitivity of different airfoil geometries to insect contamination effects are presented in Ref. 49. It is important to recognize that while sufficient insect contamination can seriously degrade airplane performance, the occurrence of serious contamination levels will be infrequent for many combinations of place, time of day, time of year, airfoil geometry, and mission profiles.

Implications of Results

These recent in-flight observations of extensive regions of NLF in the favorable pressure gradient regions on several smooth, production-quality airframes have led to a new appreciation of the operational feasibility of obtaining NLF on certain modern practical airplane surfaces. The flight experiments were conducted on eight different airplanes, including both propeller and turbojet-powered configurations and airframes constructed of aluminum or composites. The significant factor distinguishing these recent flight experiments from those of the 1930s and 1940s is the difference in preflight preparation of the surfaces tested. The recent experiments were conducted on surfaces that received (with noted exceptions) no contour or surface waviness modifications for NLF considerations. Transition Reynolds numbers ranged $1\text{-}5 \times 10^6$ for the propeller-driven airplanes and exceeded 11×10^6 for the business jet tested.

One of the objectives of the recent experiments was to determine the maximum Reynolds number range where the smoothness of modern practical airframe construction techniques will fail to meet NLF requirements in favorable pressure gradients. Based on the experimental results to date, it appears that NLF may be practical on modern production surfaces (with little sweep) for transition Reynolds numbers greater than 11×10^6. The absolute upper limit remains to be determined.

For several of the airplanes tested, comparisons were made between measured and allowable surface waviness. These comparisons showed, in general, that while the surfaces tested were not wave free, the margin between indicated and allowable waviness was favorable and significant.

Flight-measured wing profile drag for an NACA 63_2-215 airfoil on one of the composite airplanes tested with extensive laminar flow showed excellent agreement with wind-tunnel data. The effects of fixed transition on aerodynamic characteristics of several airplanes was measured. The results in all cases showed dramatic changes in performance and in some cases changes in stability and control characteristics. For the Bellanca Skyrocket II, cruise range is estimated to be increased by 25% as a benefit of laminar flow. These large effects of laminar flow on airplane aerodynamic characteristics indicate the importance of conducting fixed- and free-transition flight testing as a standard procedure for airplanes with proverse pressure gradients on surfaces smooth enough for laminar flow. This practice holds the potential for greatly improving correlation between analysis, tunnel, and flight data.

Measurement of boundary-layer transition and profiles on the wing inside the propeller slipstream on the Skyrocket indicates extensive laminar flow in this region. The data also provide information that results in a better understanding of the effects of propeller slipstreams on laminar boundary layers. A thickened, "turbulent-appearing" boundary-layer profile was measured (in a time-averaged sense) in the laminar boundary-layer region of the wing in the propeller slipstream. These recent observations suggest that previous conclusions about the loss of laminar flow in propeller slipstreams may be incorrect, since some of the early experiments mistakenly

depended on time-average-measured boundary-layer thickness or shape as an indication of transition. The implication of these observations is that the section drag increase associated with the transition changes in propeller slipstreams may not be as large as that for fixed leading-edge transition. Thus, NLF airfoils may provide drag reduction benefits, even on multiengine configurations with wing-mounted tractor engines.

The effect of wing sweep on potential leading-edge contamination was analyzed for several of the surfaces tested in flight. The results were in general agreement with a previously established empirical criterion and no obvious leading-edge contamination was observed. The experiments conducted tended to be at higher values of unit Reynolds number than would be typical for cruise. For certain relatively large lifting surfaces, business jet wings, and transport winglets, for example, spanwise contamination at cruise may not be a significant concern. Cross-flow instability is probably the principal NLF design concern for this class of swept surfaces.

Based on the recent NLF test results, maximizing the amount of laminar flow on the winglets appears very promising. Past winglet applications have made frequent use of modified airfoils from the LS(1) family [formerly the GA(W) family]. One of the factors favoring these airfoils is their desirable maximum section lift characteristics. There are two important results from recent research that should be considered in the design of future winglet airfoil sections. The first of these recent occurrences is the apparent practicality of NLF at large values of transition Reynolds numbers, and the second is the recent demonstration of the ability to design NLF airfoils with the same desirable values of high maximum section lift characteristics as obtained on the earlier low-speed turbulent flow airfoils.[53] In light of these two results, the design of special NLF airfoils for winglets should be considered.

The design constraints for a winglet NLF airfoil are considerably different from those for a wing. On a wing, the extent of laminar flow that can be designed into the airfoil is limited by pressure recovery considerations for the fully turbulent case where separation may be a problem. The same concern may not be as important for a winglet airfoil because of the relatively small effect on airplane aerodynamics due to any separation that might occasionally exist on the NLF winglet in the fully turbulent case. Thus, instead of limiting the laminar boundary-layer runs to 40-50% chord as is practical for many wing airfoils, a winglet NLF airfoil might safely support much more laminar flow. The size of the penalty for some separation in the fully turbulent case would limit the lengths of laminar runs sought. Maximum allowable pitching moment for an NLF winglet airfoil would likely be greater than for a wing, since the winglet pitching moment loads would be reacted to near the horizontal plane and, therefore, with minimized weight penalty. In addition, with no control surfaces on a winglet, aft loading due to large camber is less constrained. Thus, long laminar boundary-layer runs can be sought while maintaining the flexibility in camber constraints to meet high-lift requirements.

The potential benefit of tailoring a winglet airfoil for maximum feasible laminar boundary-layer runs results from the smaller profile drag losses the winglet must overcome to produce a net gain. With sufficiently low winglet profile drag, the lift coefficient at which drag polar crossover occurs (winglets off vs on) may be outside of the normal 1g flight envelope. A winglet with these characteristics would provide net performance gains throughout an airplane flight envelope.

For a sample insect debris contamination pattern collected on an NACA 6 series airfoil, only nine-percent of the insect strikes were of supercritical height at cruise altitude, causing transition at their locations of impact. Further studies are warranted on the combinations of airfoil geometries and mission profiles that would minimize the sensitivity to serious levels of insect debris contamination. Wind tunnel, icing tunnel, and flight experiments are planned by NASA on active systems for the protection of NLF wings against insect or ice accumulation. Such systems may be attractive for missions that allow little time between frequent landings for manual cleaning of the wing (commuter airliners, for example).

Conclusions

The following conclusions are based on the observations and measurements of boundary-layer characteristics on several modern smooth airframe surfaces:

1) The feasibility of obtaining NLF in favorable pressure gradients on certain modern practical airplane surfaces has been demonstrated for transition Reynolds numbers up to about 11×10^6.

2) Significant effects of laminar flow on airplane aerodynamics were measured by comparing free and fixed-transition test results. These large effects signify the importance of conducting fixed- and free-transition flight testing as a standard procedure for airplanes with proverse pressure gradients on surfaces smooth enough for laminar flow.

3) Significant regions of laminar flow were observed in propeller slipstreams.

4) No obvious premature transition was observed that could be attributed to excessive surface waviness. Conservative correlation was observed between empirically predicted allowable and actual waviness on the surfaces tested.

5) For a sample insect debris contamination pattern, only one-fourth of the insect strikes caused transition.

6) Fair correlation was observed between laminar flow observations on swept-wing leading edges and an empirical criterion for spanwise contamination.

References

[1] Loftin, L.K. Jr., "Subsonic Aircraft: Evolution and the Matching of Size to Performance," NASA RP-1060, 1980.

[2] Stüper, J., "Investigation of Boundary Layers on an Airplane Wing in Free Flight," NACA TM 751, 1934 (translation of "Untersuchung von Reibungsschichten am fliegenden Flugzeug," *Luftfahrtforshung*, Band 11, Nr. 1, Vol. XI, May 1934).

[3] Jones, M., "Flight Experiments on the Boundary Layer," *Journal of the Aeronautical Sciences*, Vol. 5, No. 3, Jan. 1938, pp. 81-94.

[4] Stephens, A. V. and Haslam, J.A.G., "Flight Experiments on Boundary Layer Transition in Relation to Profile Drag," British ARC R&M No. 1800, 1938.

[5] Young, A.D. and Morris, D.E., "Note on Flight Tests on the Effect of Slipstream on Boundary Layer Flow," British ARC R&M No. 1957, 1939.

[6] Young, A.D. and Morris, D.E., "Further Note on Flight Tests on the Effect of Slipstream on Boundary-Layer Flow," RAE Rept. B.A. 1404b, 1939.

[7] Young, A.D., Serby, J.E., and Morris, D.E., "Flight Tests on the Effect of Surface Finish on Wing Drag," British ARC R&M No. 2258, 1939.

[8] Goett, H.J. and Bicknell, J., "Comparison of Profile Drag and Boundary-Layer Measurements Obtained in Flight and in the Full Scale Wind Tunnel," NACA TN 693, 1939.

[9] Bicknell, J., "Determination of the Profile Drag of an Airplane Wing in Flight at High Reynolds Numbers," NACA TR 667, 1939.

[10] Wetmore, J.W., Zalovcik, J.A., and Platt, R.C., "A Flight Investigation of the Boundary Layer Characteristics and Profile Drag of the NACA 35-215 Laminar Flow Airfoil at High Reynolds Numbers," NACA WR L-532, 1941.

[11] Zalovcik, J.A., "A Profile Drag Investigation in Flight on an Experimental Fighter-Type Airplane—The North American XP-51 (Air Corps. Serial No. 41-38)," NACA ACR, Nov. 1942.

[12] Serbey, J.E., Morgan, M.B., and Cooper, E.R., "Note on Preliminary Flight Tests at High Reynolds Number of Polished and Camouflaged Painted Wing Surfaces," RAE Rept. B.A. 1315 (2588), 1936.

[13] Serbey, J.E. and Morgan, M.B., "Note on the Progress of Flight Experiments on Wing Drag," RAE Rept. B.A. 1360 (2809), 1939.

[14] Tani, I., "On the Design of Airfoils in Which the Transition of the Boundary Layer is Delayed," NACA TM 1351, 1952 (translation of "Kyo kaiso no Sen'io okuraseru Yokugata ni tuite," *Report,*

Aeronautical Research Institute, Tokyo Imperial University, No. 250, Vol. 19, Jan. 1943).

[15]Zalovcik, J.A., "Profile Drag Coefficients of Conventional and Low Drag Airfoils as Obtained In Flight," NACA WR L-139, 1944.

[16]Zalovcik, J.A. and Skoog, R.B., "Flight Investigation of Boundary Layer Transition and Profile Drag of an Experimental Low-Drag Wing Installed on a Fighter-Type Airplane," NACA WRL-94, 1945.

[17]Zalovcik, J.A., "Flight Investigation of the Boundary Layer and Profile Drag Characteristics of Smooth Wing Sections on a P-47D Airplane," NACA WRL-86, 1945.

[18]Zalovcik, J.A. and Daum, F.L., "Flight Investigation at High Speeds of Profile Drag of Wing of a P-47D Airplane Having Production Surfaces Covered With Camouflage Paint," NACA WR L-98, 1946.

[19]Plascott, R.H. "Profile Drag Measurements on Hurricane II Z.3687 Fitted With 'Low-Drag' Section Wings," RAE Rept. AERO 2153, 1946.

[20]Plascott, R.H., Higton, D.J., and Smith, F., "Flight Tests on Hurricane II Z.3687 Fitted With Special Wing of Low Drag Design," British ARC R&M No. 2546, 1946.

[21]Smith, F. and Higton, D.J., "Flight Tests on a King Cobra FZ 440 to Investigate the Practical Requirements for the Achievement of Low Profile Drag Coefficients on a 'Low Drag' Aerofoil," British ARC R&M No. 2375, 1950.

[22]Britland, C.M., "Determination of the Position of Boundary-Layer Transition on a Specially Prepared Section of Wing in Flight at Moderate Reynolds Number and Mach Number," RAE TM AERO 193, 1951.

[23]Davies, H., "Some Aspects of Flight Research," *Journal of the Royal Aeronautical Society,* June 1951.

[24]Gray, W.E. and Davies, H., "Note on the Maintenance of Laminar Flow Wings," British ARC R&M No. 2485, 1952.

[25]Montoya, L.C., Steers, L.L., Christopher, D., and Trujillo, B., "Natural Laminar Flow Glove Flight Results," NASA CP-2208, 1981, pp. 11-20.

[26]Banner, R.D., McTigue, J.G., and Petty, G., Jr., "Boundary Layer Transition Measurements in Full Scale Flight," NACA RM H58E28, 1958.

[27]"Final Report on LFC Aircraft Design Data Laminar Flow Control Demonstration Program," Northrop Corp., Rept. NOR 67-136 [Contract AF33(657)-13930], June 1967 (available from DDC as AD 819 317).

[28]Bushnell, D.M. and Tuttle, M. H., "Survey and Bibliography on Attainment of Laminar Flow Control in Air Using Pressure Gradient and Suction," NASA RP-1035, Vol. 1, 1979.

[29]Hood, M.J. and Gaydos, M.E., "Effects of Propellers and Vibration on the Extent of Laminar Flow on the NACA 27-212 Airfoil," NACA ACR (WR L-784), 1939.

[30]Holmes, B.J., Yip, L.P., and Obara, C.J., "Observations of National Laminar Flow on Modern Airplane Surfaces," NASA TP 2256, 1984.

[31]Holmes, B.J., Obara, C.J., Gregorek, G.M., Hoffman, M.J., and Freuler, R.J., "Flight Investigation of Natural Laminar Flow on the Bellanca Skyrocket II," SAE Paper 830717, 1983.

[32]Pringle, G.E. and Main-Smith, J.D., "Boundary Layer Transition Indicated by Sublimation," RAE Tech. Note AERO 1652 (ARC 8892), 1945.

[33]Main-Smith, J.D., "Chemical Solids as Diffusible Coating Films for Visual Indication of Boundary Layer Transition in Air and Water," British ARC R&M No. 2755, 1950.

[34]Owen, P.R. and Ormerod, A.O., "Evaporation From the Surface of a Body in an Airstream," British ARC R&M No. 2875, 1951.

[35]Braslow, A.L. and Knox, E.C., "Simplified Method for Determination of Critical Height of Distributed Roughness Particles for Boundary Layer Transition at Mach Numbers from 0 to 5," NACA TN 4363, 1958.

[36]Stevens, W.A., Goradia, S.H., and Braden, J.A., "Mathematical Model for Two-Dimensional Multi-Component Airfoils in Viscous Flow," NASA CR-1843, 1971.

[37]Abbott, I.H., von Doenhoff, A.E., and Stivers, L.S., Jr., "Summary of Airfoil Data," NACA TR-824, 1945.

[38]Gregorek, G.M., Hoffman, M.J., Payne, H., and Harris, J.P., "Drag Evaluation of the Bellanca Skyrocket II," SAE Paper 770472, 1977.

[39]Wenzinger, C.J., "Wind Tunnel Investigation of Several Factors Affecting the Performance of a High Speed Pursuit Airplane with Air-Cooled Engine," NACA ACR, Nov. 1941.

[40]Holmes, B.J. and Obara, C.J., "Observations and Implications of Natural Laminar Flow on Practical Airplane Surfaces," ICAS Paper 82-5.1.1, 1982.

[41]Beasley, J.A., "Calculation of the Laminar Boundary Layer and Prediction of Transition on a Sheared Wing," British ARC R&M No. 3787, 1976.

[42]Gilkey, R.D., "Design and Wind Tunnel Tests of Winglets on a DC-10 Wing," NASA CR-3119, 1979.

[43]Glick, P.A., "The Distribution of Insects, Spiders and Mites in the Air," U.S. Dept. of Agriculture, Tech. Bull. 673, 1939.

[44]Freeman, J.A., "Studies in the Distribution of Insects by Aerial Currents: The Insect Population in the Air from Ground Level to 300 Feet," *Journal of Animal Ecology,* Vol. 14, 1945, pp. 128-154.

[45]Atkins, P.B., "Wing Leading Edge Contamination by Insects," ARL (Australia) Flight Note 17, Oct. 1951.

[46]Johnson, D., "Brief Measurements of Insect Contamination on Aircraft Wings," ARC TR 14999, May 1952.

[47]Lachmann, G.V., "Aspects of Insect Contamination in Relation to Laminar Flow Aircraft," HMSO, London, C.P. 484, 1960.

[48]Coleman, W.S., "Roughness Due to Insects. Boundary Layer and Flow Control—Its Principles and Application," Vol. 2, Pergamon Press, New York, 1961.

[49]Boermanns, L.M.M. and Selen, H.J.W., "On the Design of Some Airfoils for Sailplane Application," Dept. of Aerospace Engineering, Delft University of Technology, April 1981.

[50]Kohlman, D.L., "Icing Tunnel Tests of a Glycol-Exuding Porous Leading Edge Ice Protection System on a General Aviation Airfoil," NASA CR-165444, 1981.

[51]"Evaluation of Laminar Flow Control System Concepts for Subsonic Commercial Transport Aircraft," NASA CR-159253, 1980.

[52]Peterson, J.B. Jr. and Fisher, D.F., "Flight Investigation of Insect Contamination and Its Alleviation," NASA CP-2036, 1978, pp. 357-374.

[53]Somers, D.M., "Design and Experimental Results for a Natural Laminar Flow Airfoil for General Aviation Applications," NASA TP-1861, 1981.